Fermi surface reconstruction and dimensional topology change in Nd-doped CeCoIn$_5$

J. Klotz,[1,2] K. Götze,[1,2,*] I. Sheikin,[3] T. Förster,[1] D. Graf,[4] J.-H. Park,[4] E. S. Choi,[4]
R. Hu,[5] C. Petrovic,[5] J. Wosnitza,[1,2] and E. L. Green[1,†]

[1]*Hochfeld-Magnetlabor Dresden (HLD-EMFL), Helmholtz-Zentrum Dresden-Rossendorf, D-01328 Dresden, Germany*
[2]*Institut für Festkörper- und Materialphysik, Technische Universität Dresden, D-01069 Dresden, Germany*
[3]*Laboratoire National des Champs Magnétiques Intenses (LNCMI-EMFL), CNRS, UGA, F-38042 Grenoble, France*
[4]*National High Magnetic Field Laboratory, Florida State University, Tallahassee, Florida 32310, USA*
[5]*Condensed Matter Physics and Materials Science Department, Brookhaven National Laboratory, Upton, New York 11973, USA*

We performed low-temperature de Haas–van Alphen effect measurements on a $Ce_{1-x}Nd_xCoIn_5$ series, for $x = 0.02$, 0.05, 0.1, and 1, down to $T = 40$ mK using torque magnetometry in magnetic fields up to 35 T. Our results indicate that a Fermi surface (FS) reconstruction occurs from a quasi-two-dimensional topology for Nd-2% to a rather three-dimensional one for Nd-5%, thus reducing the possibility of perfect FS nesting. The FS evolves further with increasing Nd content with no observed divergence of the effective mass between Nd-2% and 10%, consistent with the crossing of a spin density wave type of quantum critical point. Our results elucidate the origin of the Q phase observed at the 5% Nd-doping level [Raymond *et al.*, J. Phys. Soc. Jpn. **83**, 013707 (2014)].

Heavy-fermion systems have garnered attention over the past few decades due to their novel physical properties and exotic behavior, particularly when exposed to high magnetic fields [1–4]. Most notably CeCoIn$_5$, which has the highest critical temperature of all Ce-based heavy-fermion compounds ($T_c = 2.3$ K [5,6]), exhibits a field-induced ordered phase from 10 up to 11.4 T for $B \parallel a$ [7], a superconducting state now referred to as the Q phase. It was initially believed this high-field state was the realization of the long-sought-after Fulde-Ferrell Larkin-Ovchinnikov (FFLO) phase [7–10], however, further measurements revealed the presence of antiferromagnetic (AFM) order [11–13]. Many questions, however, still remain about the interactions appearing in this high-field superconducting state.

By substituting a portion of the Ce atoms in CeCoIn$_5$ with Nd, an atom where the $4f$ electrons do not hybridize with the conduction electrons, one can introduce a spin density wave (SDW) and, at higher Nd contents, AFM order [14,15]. It was recently reported that by replacing 5% of the Ce atoms with Nd, the high-field Q phase could be stabilized at zero applied magnetic field, inciting intense research to explore the mechanism behind such unique properties [14,16–18]. An enhancement of the nesting has been proposed [14], however, experimental proof has been insufficient, thus providing our motivation to explore how Nd alters the Fermi surface (FS). Additionally, it has previously been suggested that a quantum critical point (QCP) may exist in these materials [16], which may also be induced by increasing Nd doping [15].

In this Rapid Communication, we provide evidence for a drastic FS reconstruction between 2% and 5% Nd substitution.

The reconstruction manifests itself in a sharp deviation of the α orbit from the expected $1/\cos\theta$ dependence normally associated with a quasi-two-dimensional (2D) cylindrical FS. This is at odds with assumptions made in current theoretical models [19]. Furthermore, this distorted FS may be described as more 3D in nature and any effects from possible FS nesting suggested in prior works [14] may, therefore, be significantly reduced. The FSs continue to evolve for 5%, 10%, and 100% Nd substitution and are consistent with fully localized $4f$ electrons only at 100% substitution. The effective mass associated with the quasi-2D cylindrical band, previously found to play a key role in superconductivity [20,21], remains constant between 0% and 10% Nd substitution levels. Both the progressive change of the FSs with increasing substitution level and nondivergent effective carrier masses indicate the SDW-type nature of the QCP [22,23], consistent with thermodynamic measurements [15].

High-quality single crystals of $Ce_{1-x}Nd_xCoIn_5$ with $x = 0.02$, 0.05, 0.1, and 1 (herein referred to as Nd-2%, 5%, 10%, and 100%) were grown and characterized as described elsewhere [15]. Torque magnetometry was performed at the Laboratoire National des Champs Magnétiques Intenses (LNCMI) in Grenoble, France, and the National High Magnetic Field Laboratory (NHMFL) in Tallahassee, USA, using a capacitive beam cantilever mounted on a rotator and placed in a top-loading ^{3}He/^{4}He dilution refrigerator. To accurately probe the lighter effective masses in NdCoIn$_5$, a ^{3}He cryostat was utilized. Band-structure calculations for NdCoIn$_5$ were performed using the full-potential local-orbital (FPLO) minimum-basis code (version 9.01-35) [24] with a scalar-relativistic setting and the local density approximation of Ref. [25]. Lattice parameters were taken from Ref. [26].

The de Haas–van Alphen (dHvA) oscillations were detected using field-dependent torque magnetometry (21–35 T) for Nd-2%, 5%, 10%, and 100%, but could not be resolved for

---

*Present address: Department of Physics, University of Warwick, Coventry CV4 7AL, United Kingdom.
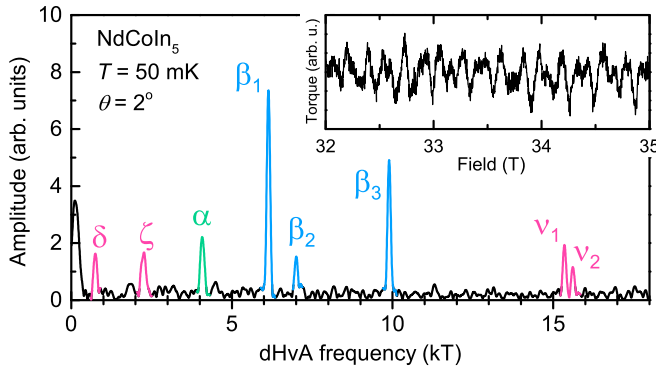
†e.green@hzdr.de

FIG. 1. Fourier transform of the quantum oscillations between 21 and 35 T measured on NdCoIn$_5$ at an angle $\theta = 2°$ from [001] to [110]. The inset shows the torque signal at high magnetic fields after background subtraction.

midrange substitution levels (Nd-20% and 60%). Background magnetization was subtracted using a higher-order polynomial fit, resulting in oscillations as shown for NdCoIn$_5$ in the inset of Fig. 1. A Fourier transform revealed several prominent frequencies well above the noise level (see Fig. 1). The angular dependence for the dHvA frequencies was explored, rotating from $B \parallel c$ ([001]) to $B \perp c$ ([100]), for Nd-2%, 5%, and 10%, as shown in Figs. 2(a)–2(c). Nd-100% was rotated towards [110] [see Fig. 2(d)]. In pure CeCoIn$_5$, it has been shown that there is little difference in the dHvA frequencies between [100] and [110] due to the mostly isotropic FSs in the a-b plane

[27,28]. The same is assumed to be true for the isostructural compound NdCoIn$_5$, backed by our calculations.

Numerous frequencies could be resolved for Nd-2%, as shown in Fig. 2(a), many of which correspond to those found in CeCoIn$_5$ [27,29]. The frequency labeled β by Settai *et al.* [28] could not be observed, possibly due to increased impurity scattering, which affects heavy-mass orbits more strongly. Instead, we observe frequencies of 6.25 and 6.92 kT at $\theta = 3°$, which were not reported for pure CeCoIn$_5$ [27–30]. Since the frequencies between 4 and 8 kT, labeled α, follow roughly a $1/\cos\theta$ dependence, where θ is the angle between the applied magnetic field and the c direction (see the drawing in Fig. 4), it is plausible that these frequencies arise from a strongly corrugated 2D cylindrical FS.

A drastic FS reconstruction occurs for 5% Nd doping [Fig. 2(b)]. The frequencies ϵ and γ in Nd-2% disappear and are replaced by δ and ζ in Nd-5%. Frequencies associated with the α orbits noticeably deviate from the expected $1/\cos\theta$ dependence seen in the 2% Nd-doping level, indicating the 2D cylindrical FS has now warped into more of a quasi-3D structure. This is of particular interest because recent theoretical work exploring the reasoning behind the appearance of the Q phase at zero applied magnetic field is based on the assumption that doping has a negligible effect on the FS [19]. Furthermore, it has been proposed that the Q vector appears at 0 T due to an enhanced FS nesting [14]. However, since the cylindrical FS is developing a more 3D structure, this scenario seems unlikely.

As the substitution level increases to 10%, the frequencies associated with the δ and ζ continue to evolve [Fig. 2(c)].
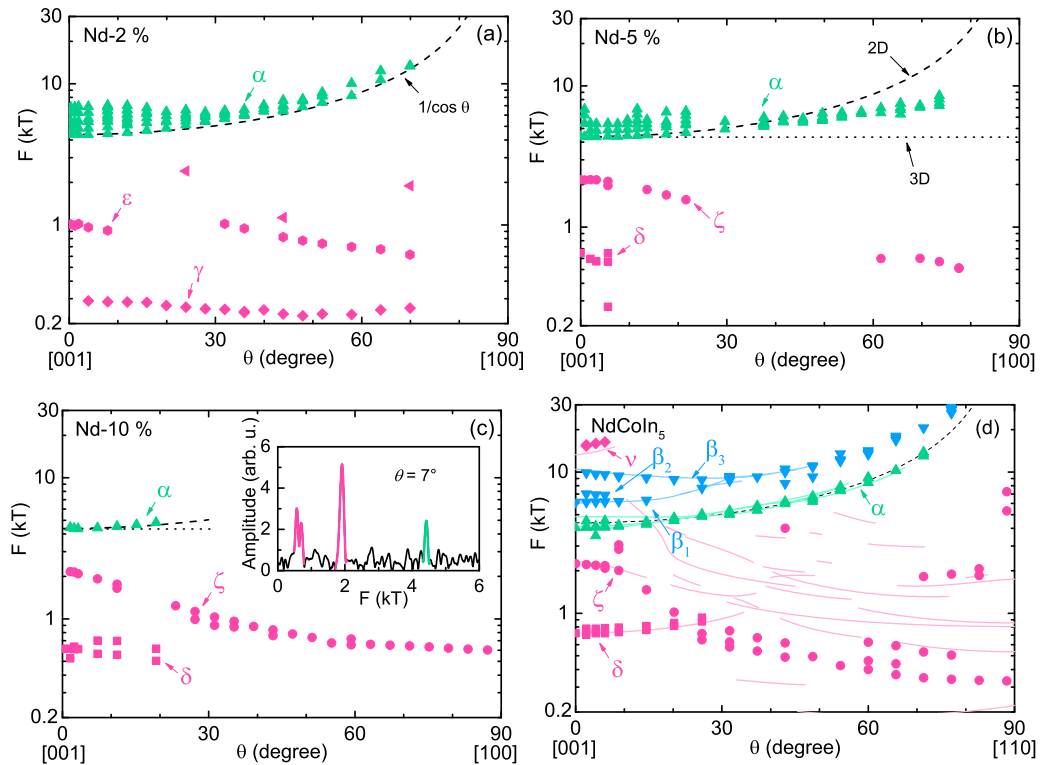

FIG. 2. Angular dependence of the dHvA frequencies for (a) Nd-2%, (b) 5%, (c) 10%, and (d) 100%. The latter includes the results of the band-structure calculations, shown as lines. The labeling of the frequency branches has been defined so as to be consistent with prior works [27,30]. Dashed lines denote $1/\cos\theta$ dependence arising from a 2D cylindrical FS, dotted from a 3D sphere. The inset in (c) depicts the fast Fourier transform (FFT) for $\theta = 7.2°$.
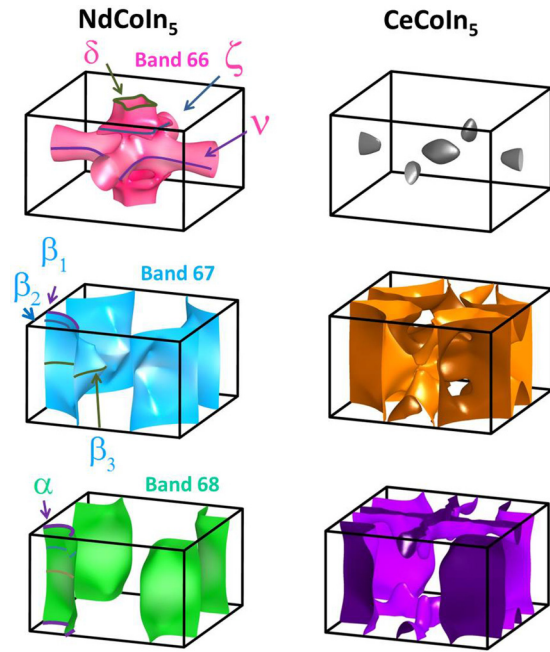
FIG. 3. Calculated FSs for NdCoIn$_5$ (left) and CeCoIn$_5$ (right). The black frames depict the first Brillouin zone. The solid lines on the FSs aid in the visualization of some extremal orbits for the magnetic field aligned along the c axis. For NdCoIn$_5$ (left), 66 is a hole band while 67 and 68 are electron bands.

Few frequencies associated with the α band could be seen, all agreeing with frequencies found for Nd-2% and Nd-5%. Due to increased scattering provoked by doping-induced disorder, quantum oscillations could not be detected for further substitution levels (20% and 60%), but numerous frequencies appear for NdCoIn$_5$ as seen in Fig. 2(d). Furthermore, a well-defined 2D cylindrical FS, labeled α as before, reemerges, as evidenced by the $1/\cos\theta$ behavior, but with a different FS cross section. In addition, a second corrugated 2D cylindrical FS labeled β is identified by a $1/\cos\theta$ dependence.

Band-structure calculations for NdCoIn$_5$, performed assuming localized, nonhybridizing $4f$ electrons, are in good agreement with experimental data [see Fig. 2(d)]. The topology of the FSs for NdCoIn$_5$ along with their corresponding frequencies are depicted in Figs. 2(d) and 3, herein referred to as band 66, band 67, and band 68, represented in the graphs as pink, blue, and green, respectively. A comparison between the FSs of CeCoIn$_5$ and NdCoIn$_5$ is shown in Fig. 3. As a note, the FS could only reasonably be calculated for NdCoIn$_5$ and CeCoIn$_5$, not for the substitution series because of the increased complexity doping introduces to the calculation.

Effective masses were extracted by fitting the oscillation amplitudes, shown in Fig. 4, to the Lifshitz-Kosevich formula [31,32]. In order to observe a sufficiently strong torque signal for as many frequency branches as possible, effective masses were measured at angles between 4° and 10° from the c axis for the different substitution levels. Effective masses for the observed frequencies in NdCoIn$_5$ are shown in Table I and are slightly larger than the calculated masses reflecting modest mass enhancements quantified by $\lambda = m^*/m_b - 1$ [36]. Effective masses for all other substitution levels are shown
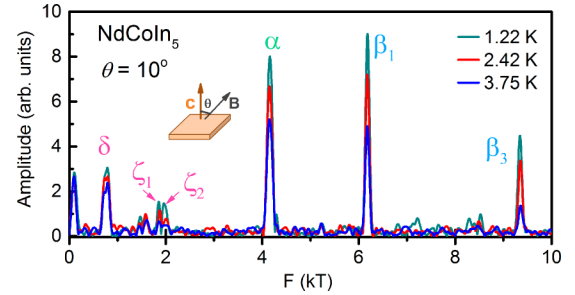

FIG. 4. Example of the temperature dependence of the observed frequencies in NdCoIn$_5$ measured between 21 and 35 T at an angle of $\theta = 10°$ from [001] to [110].

in Table II. It is evident that increasing the substitution level has little effect on the effective masses of existing orbits up to Nd-10%, while newly appearing orbits have a greatly reduced mass.

The effective mass for α_3, the orbit associated with the 2D band at low doping level and the only branch that can be tracked up to Nd-10%, remains relatively unchanged with increasing substitution levels despite T_c rapidly decreasing ($T_c = 2.1$, 2.0, and 1.8 K for Nd-2%, 5%, and 10%, respectively) [15]. This behavior near QCPs was observed in the CeRh$_{1-x}$Co$_x$In$_5$ [37] and CeCo(In$_{1-x}$Cd$_x$)$_5$ [38] series, but differs from the Ce$_x$La$_{1-x}$CoIn$_5$ [39] series and the pressure-induced QCP in CeRhIn$_5$ [40]. Consequently, our data indicate the presence of a SDW-type QCP [22,23], consistent with the experimental phase diagram [15]. The cylindrical FSs are generally assumed to be the heavy bands that possess the largest energy gap [20] and are theoretically considered to experience the interacting pairing potential relevant for superconductivity [41]. Therefore, since the band remains relatively heavy, most probably due to electronic correlations, Nd is likely altering the pairing potential. This is in agreement with the reduced jump in the specific heat upon entering the superconducting state [15].

In conclusion, the FS of Ce$_{1-x}$Nd$_x$CoIn$_5$ changes across the QCP associated with the appearance of long-range magnetic order at Nd-5% and continues to evolve with increasing x, consistent with a SDW-type QCP [22,23]. Furthermore, between Nd-2% and Nd-5%, the FS moves away from two-dimensionality which is at odds with an enhanced Fermi-nesting scenario given as an explanation for the Q phase seen at zero applied magnetic field [14]. Since effective masses are unaffected by altering Nd content up to 10% despite a

TABLE I. Comparison of effective masses measured at an angle of 10° from [001] to [110] of NdCoIn$_5$ with calculations.

Branch	Experiment		Calculation		λ
	F (kT)	m^* (m_e)	F (kT)	m_b (m_e)	$m^*/m_b - 1$
δ	0.79	0.53(8)	0.74	0.29	0.82
ζ_1	1.87	1.0(2)			
ζ_2	1.98	1.2(2)			
α	4.15	0.83(3)	4.12	0.73	0.13
β_1	6.17	1.06(3)	6.18	0.77	0.37
β_3	9.36	1.3(2)	9.42	0.86	0.55

TABLE II. Effective masses for the various frequencies depicted in Figs. 3(a)–3(c). Frequencies and effective masses associated with CeCoIn$_5$ were taken from Ref. [30]. m^* associated with α remains relatively stable with increased Nd doping.

Branch	CeCoIn$_5$ [30] $\theta = 0°$		Nd-2% $\theta = 3°$		Nd-5% $\theta = 2°$		Nd-10% $\theta = 7°$	
	F (kT)	m^* (m_e)	F (kT)	m^* (m_e)	F (kT)	m^* (m_e)	F (kT)	m^* (m_e)
γ			0.29	6.4(6)				
ϵ			0.99	20.3(15)				
δ_1					0.59	<1	0.55	<1
δ_2							0.68	<1
ζ					2.16	<1	1.9	<1
α_1	5.46	14.5	5.44	10.3(5)	5.42	10.0(5)		
α_2	4.87	11.4	4.85	11.0(5)	4.84	10.5(8)		
α_3	4.37	9.3	4.39	6.7(2)	4.38	6.8(2)	4.41	7(1)
α_4			6.25	12.0(10)				
α_5			6.92	18.5(7)				

decrease in T_c, it is plausible to conclude that Nd alters the electronic pairing potential. Our results provide information on the evolution of the FS topology under Nd perturbation and its influence on the emerging Q phase in Nd-5%.

[1] I. Kouroudis, D. Weber, M. Yoshizawa, B. Lüthi, L. Puech, P. Haen, J. Flouquet, G. Bruls, U. Welp, J. J. M. Franse, A. Menovsky, E. Bucher, and J. Hufnagl, Phys. Rev. Lett. **58**, 820 (1987).

[2] D. M. Edwards and A. C. M. Green, Z. Phys. B **103**, 243 (1997).

[3] H. von Löhneysen, J. Phys.: Condens. Matter **8**, 9689 (1996).

[4] D. K. Singh, A. Thamizhavel, J. W. Lynn, S. Dhar, J. Rodriguez-Rivera, and T. Herman, Sci. Rep. **1**, 117 (2011).

[5] C. Petrovic, P. G. Pagliuso, M. F. Hundley, R. Movshovich, J. L. Sarrao, J. D. Thompson, Z. Fisk, and P. Monthoux, J. Phys.: Condens. Matter **13**, L337 (2001).

[6] S. Ikeda, H. Shishido, M. Nakashima, R. Settai, D. Aoki, Y. Haga, H. Harima, Y. Aoki, T. Namiki, H. Sato, and Y. Ōnuki, J. Phys. Soc. Jpn. **70**, 2248 (2001).

[7] A. Bianchi, R. Movshovich, C. Capan, P. G. Pagliuso, and J. L. Sarrao, Phys. Rev. Lett. **91**, 187004 (2003).

[8] P. Fulde and R. A. Ferrell, Phys. Rev. **135**, A550 (1964).

[9] A. I. Larkin and Yu. N. Ovchinnikov, Zh. Eksp. Teor. Fiz. **47**, 1136 (1964) [Sov. Phys. JETP **20**, 762 (1965)].

[10] H. A. Radovan, N. A. Fortune, T. P. Murphy, S. T. Hannahs, E. C. Palm, S. W. Tozer, and D. Hall, Nature (London) **425**, 51 (2003).

[11] V. F. Mitrović, M. Horvatić, C. Berthier, G. Knebel, G. Lapertot, and J. Flouquet, Phys. Rev. Lett. **97**, 117002 (2006).

[12] B.-L. Young, R. R. Urbano, N. J. Curro, J. D. Thompson, J. L. Sarrao, A. B. Vorontsov, and M. J. Graf, Phys. Rev. Lett. **98**, 036402 (2007).

[13] M. Kenzelmann, Th. Strässle, C. Niedermayer, M. Sigrist, B. Padmanabhan, M. Zolliker, A. D. Bianchi, R. Movshovich, E. D. Bauer, J. L. Sarrao, and J. D. Thompson, Science **321**, 1652 (2008).

[14] S. Raymond, S. M. Ramos, D. Aoki, G. Knebel, V. P. Mineev, and G. Lapertot, J. Phys. Soc. Jpn. **83**, 013707 (2014).

[15] R. Hu, Y. Lee, J. Hudis, V. F. Mitrovic, and C. Petrovic, Phys. Rev. B **77**, 165129 (2008).

[16] D. G. Mazzone, S. Raymond, J. L. Gavilano, E. Ressouche, C. Niedermayer, J. O. Birk, B. Ouladdiaf, G. Bastien, G. Knebel, D. Aoki, G. Lapertot, and M. Kenzelmann, Sci. Adv. **3**, e1602055 (2017).

[17] D. G. Mazzone, S. Raymond, J. L. Gavilano, P. Steffens, A. Schneidewind, G. Lapertot, and M. Kenzelmann, Phys. Rev. Lett. **119**, 187002 (2017).

[18] D. G. Mazzone, R. Yadav, M. Bartkowiak, J. L. Gavilano, S. Raymond, E. Ressouche, G. Lapertot, and M. Kenzelmann, Sci. Rep. **8**, 1295 (2018).

[19] J. H. J. Martiny, M. N. Gastiasoro, I. Vekhter, and B. M. Andersen, Phys. Rev. B **92**, 224510 (2015).

[20] M. P. Allan, F. Massee, D. K. Morr, J. Van Dyke, R. W. Rost, A. P. Mackenzie, C. Petrovic, and J. C. Davis, Nat. Phys. **9**, 468 (2013).

[21] K. Götze, J. Klotz, D. Gnida, H. Harima, D. Aoki, A. Demuer, S. Elgazzar, J. Wosnitza, D. Kaczorowski, and I. Sheikin, Phys. Rev. B **92**, 115141 (2015).

[22] Q. Si and F. Steglich, Science **329**, 1161 (2010).

[23] P. Gegenwart, Q. Si, and F. Steglich, Nat. Phys. **4**, 186 (2008).

[24] K. Koepernik and H. Eschrig, Phys. Rev. B **59**, 1743 (1999).

[25] J. P. Perdew and Y. Wang, Phys. Rev. B **45**, 13244 (1992).

[26] J. Hudis, R. Hu, C. L. Broholm, V. F. Mitrovic, and C. Petrovic, J. Magn. Magn. Mater. **307**, 301 (2006).

[27] D. Hall, E. C. Palm, T. P. Murphy, S. W. Tozer, Z. Fisk, U. Alver, R. G. Goodrich, J. L. Sarrao, P. G. Pagliuso, and T. Ebihara, Phys. Rev. B **64**, 212508 (2001).

[28] R. Settai, H. Shishido, S. Ikeda, Y. Murakawa, M. Nakashima, D. Aoki, Y. Haga, H. Harima, and Y. Ōnuki, J. Phys.: Condens. Matter **13**, L627 (2001).

[29] H. Shishido, T. Ueda, S. Hashimoto, T. Kubo, R. Settai, H. Harima, and Y. Ōnuki, J. Phys.: Condens. Matter **15**, L499 (2003).

[30] A. Polyakov, O. Ignatchik, B. Bergk, K. Götze, A. D. Bianchi, S. Blackburn, B. Prévost, G. Seyfarth, M. Côté, D. Hurt, C. Capan, Z. Fisk, R. G. Goodrich, I. Sheikin, M. Richter, and J. Wosnitza, Phys. Rev. B **85**, 245119 (2012).

[31] D. Shoenberg, *Magnetic Oscillations in Metals* (Cambridge University Press, Cambridge, UK, 1984).

[32] See Supplemental Material at http://link.aps.org/supplemental/10.1103/PhysRevB.98.081105 for discussions of the energy bands from the band-structure calculations, a detailed description of how the effective mass was extracted, and the possible reasons behind the discrepancy between the Sommerfeld coefficients extracted from prior specific heat measurements and the effective masses found in this work, which includes Refs. [33,34,35].

[33] G. Zwicknagl, Rep. Prog. Phys. **79**, 124501 (2016).

[34] P. Thalmeier and G. Zwicknagl, in *Handbook on the Physics and Chemistry of Rare Earths*, edited by K. A. Gschneidner, Jr., J.-C. Bünzli, and V. Pecharsky (North-Holland, Amsterdam, 2004), Vol. 34, pp. 135–287.

[35] A. McCollam, S. R. Julian, P. M. C. Rourke, D. Aoki, and J. Flouquet, Phys. Rev. Lett. **94**, 186401 (2005).

[36] FPLO typically results in lower effective masses than are observed experimentally, as is the case here, because it does not take many-body interactions into account.

[37] S. K. Goh, J. Paglione, M. Sutherland, E. C. T. O'Farrell, C. Bergemann, T. A. Sayles, and M. B. Maple, Phys. Rev. Lett. **101**, 056402 (2008).

[38] C. Capan, Y.-J. Jo, L. Balicas, R. G. Goodrich, J. F. DiTusa, I. Vekhter, T. P. Murphy, A. D. Bianchi, L. D. Pham, J. Y. Cho, J. Y. Chan, D. P. Young, and Z. Fisk, Phys. Rev. B **82**, 035112 (2010).

[39] N. Harrison, U. Alver, R. G. Goodrich, I. Vekhter, J. L. Sarrao, P. G. Pagliuso, N. O. Moreno, L. Balicas, Z. Fisk, D. Hall, R. T. Macaluso, and J. Y. Chan, Phys. Rev. Lett. **93**, 186405 (2004).

[40] H. Shishido, R. Settai, H. Harima, and Y. Ōnuki, J. Phys. Soc. Jpn. **74**, 1103 (2005).

[41] J. S. Van Dyke, F. Massee, M. P. Allan, J. C. Séamus Davis, C. Petrovic, and D. K. Morr, Proc. Natl. Acad. Sci. USA **111**, 11663 (2014).